Send Orders of Reprints at reprints@benthamscience.net

Current Organic Chemistry, 2013, *17*, 65-71

A Method for the Micro-encapsulation of Dielectric Fluids in Joined Polymer Shells

Catherine Tonry[1*], Mayur K. Patel[1], Christopher Bailey[1], Marc P.Y. Desmuliez[2], Scott Cargill[2] and Weixing Yu[3]

[1]*Computational Mechanics and Reliability Group (CMRG), School of Computing and Mathematical Sciences, University of Greenwich, 30 Park Row, London SE10, 9LS, UK*

[2]*Microsystems Engineering Centre (MISEC), School of Engineering & Physical Sciences, Heriot-Watt University, Earl Mountbatten Building, Edinburgh EH14 4AS, UK*

[3]*State Key Laboratory of Applied Optics, Changchun Institute of Optics, Fine mechanics and Physics, Chinese Academy of Sciences, 3888 Dongnanhu Road, Changchun, Jilin, P. R. China*

Abstract: Electric Field Assisted Capillarity (EFAC) is a novel manufacturing technique that allows for the one-step fabrication of enclosed microstructures, such as microchannels and microcapsules. After a brief review of current micro-encapsulation techniques, this paper presents a list of potential applications for this technology; what is currently known about its mechanisms and avenues for further research.

Keywords: Microcapsules, Microstructures, Microfluidics.

INTRODUCTION

There are several current manufacturing techniques for microcapsules which usually involve the manufacture of spheres of encapsulated fluids. These methods include the encapsulation of enzymes in cellulose nitrate membranes or polyamide membranes [1], the encapsulation of cells in alginate gels [1] collagen, chitosan, or agarose [2]. This paper however presents and discusses a novel method for micro-encapsulation of dielectric fluids within polymer shells, which are joined together in a single step process [3]. This direct encapsulation method is currently not possible with current technologies. To achieve a similar effect using present processes, microcapsules would have to be bonded to a substrate after manufacture. This gives a random array of capsules which are not necessarily the same size.

The fabrication technique, known as Electric Field Assisted Capillarity (EFAC), uses a combination of the dielectric and surface tension properties of a polymer combined with a heavily wetted surface to create fully enclosed microstructures [3]. These microstructures can enable the production of enclosed microchannels, microcapsules or a combination of both in a single step process. It has potential advantages over other methods in that the capsules produced are both of similar sizes and can be arranged in a beneficial pattern.

APPLICATIONS

Although the fabrication method is still in its infancy, initial experimental results and numerical results have been very encouraging for potential applications.

The technique may have potential uses in building layers of microcapsules for slow release drug delivery, and could produce comparable systems to those described by Sata *et al.* [4]. The paper also describes both the use of microcapsules and of layers of LbL films to entrap the molecules. Similarly LbL films that are sensitive to heat [5] or ultrasound [5] have also been produced. Using the EFAC process layers of microcapsules could be produced using similar materials producing a similar effect.

Another potential application of the EFAC fabrication method would be in the manufacture of a bioartificial pancreas. Using a partially permeable polymer combined with the EFAC technique it could be possible to construct an array of partially permeable microcapsules, combined with arrays of microchannels. The partially permeable capsules could contain islets of Langerhans and insulin releasing endocrine tissue, which would be protected from antibodies and thus immune response by the partially permeable membrane. The membrane would however allow insulin and waste products out of the capsules; and allow oxygen, glucose and other required nutrients in. Using these microcapsules it would be possible to fabricate a bioartifical pancreas such as those described by Teramura and Iwata [6].

Further applications include the fabrication of arrays of microchannels for use in microfluidic devices. Alternative methods usually involve multiple process steps and are therefore more costly [7]. Other applications include the manufacturing of microlens arrays similar to those described by Xia *et al.* [8] or the fabrication of optical waveguides [9].

ENCAPSULATING DIELECTRIC FLUIDS

Electric Field Assisted Capillarity (EFAC) is an extension of the Lithographically Induced Self Assembly (LISA) and Lithgoraphically Induced Self Construction (LISC) techniques. LISA was initially described by Chou and Zhuang [10], whereby a thin homopolymer film was placed between two electrodes. The polymer is then heated to just above its glass transition temperature so it becomes softened, alternatively an ultra violet curable polymer can be used prior to curing. An electric field is then applied to the viscous polymer. The Coulombic force exerted on the polymer surface creates instabilities on the surface of the film and the polymer begins to grow upwards towards the mask thereby creating an array of uniform columns. Lin *et al.* [12] looked into the process when ap-

*Address correspondence to this author at the Computational Mechanics and Reliability Group (CMRG), School of Computing and Mathematical Sciences, University of Greenwich, 30 Park Row, London SE10, 9LS, UK; Tel: +44 (0)20 8331 7796; Fax: +44 (0)20 8331 8665; E-mail: C.E.Tonry@greenwich.ac.uk

1385-2728/13 $58.00+.00

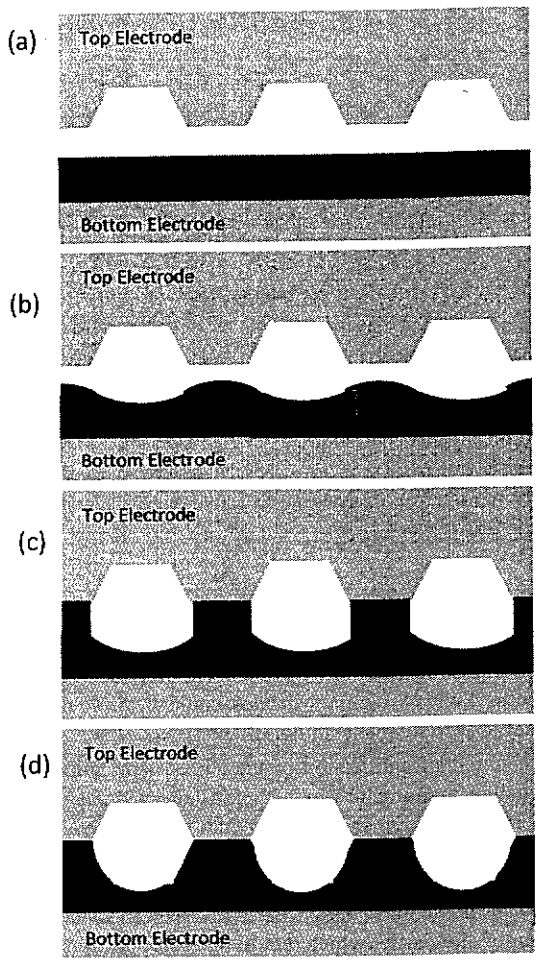

Fig. (1). Schematic of the Lithographically Induced Self Construction (LISC) process. The dark (gradient) region is the polymer.

plied to polymer liquid interfaces and found that the length scale of the instabilities was reduced compared to the case of a polymer air interface. There have been several theoretical studies into this process, the first study by Suo and Liang [13] looked at the instabilities which cause the initial protrusions from the polymer. These protrusions then experience a greater electrostatic force than the areas around them, which causes them to grow upwards creating the columns seen in Lithographically Induced Self Assembly.

Lithographically Induced Self-Construction (LISC) is an extension of the LISA process and allows a copy of a shaped top mask to be produced in the polymer allowing for the construction of open microstructures in a reliable non-contact process [11]. LISC uses an electric field that shapes a polymer to produce a replica of a top mask. A schematic of this process can be seen in Fig. (**1**), where a viscous polymer is placed initially between two electrodes (a). The dielectric forces at the surface then cause a larger force on the polymer in areas of high electric field, as the magnitude of the force is proportional to the square of the electric field. This causes the polymer to flow towards the top electrode in these regions (b). The polymer then must flow away from the mask in areas of low electric field magnitude. When the polymer reaches the top mask (c) it can no longer move upwards and so the electrostatic forces combined with surface tension cause a channel to be formed (d). If there is the correct quantity of polymer so it mostly depletes flat bottomed microstructures are able to be formed.

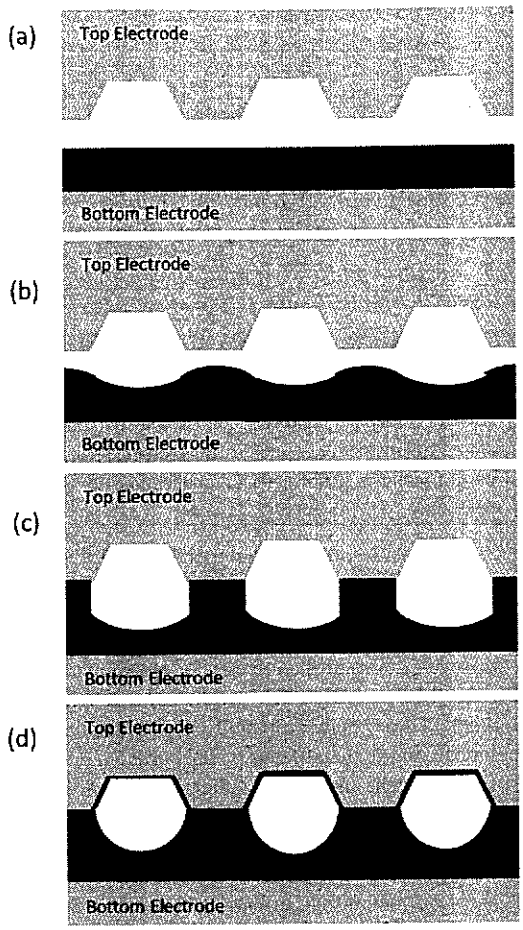

Fig. (2). Schematic of the Electric Field Assisted Capillarity (EFAC) process. The dark (gradient) region is the polymer.

Electric Field Assisted Capillarity (EFAC) extends this concept by using a heavily wetted top mask. This means that the top mask is such that it is very hydrophilic to the polymer and so the polymer has a very low contact angle to the mask causing large capillary force [3]. A diagram of the process can be seen in Fig. (**2**). The process starts in the same way with a thin film of viscous polymer between two electrodes (a). A potential difference is applied between the two electrodes. This results in areas of higher electric field causing the polymer to flow towards the top mask (b). The process differs from LISC when the polymer reaches the top mask (c). As the top mask is heavily wetted there is a large capillary force, caused by the small contact angle, this capillary force being greater than the cohesive force due to the comparibly low surface tension of the polymer combined with the lowering of the surface tension caused by the voltage close to the electrode (Lipmann effect). For a sufficiently small contact angle, the force causes the polymer to flow around the top mask forming a shell and thus fully enclosing the fluid inside (d).

The experiments performed with this process have so far only been performed with polydimethylsiloxane (PDMS). However, any dielectric polymer with a comparatively low surface tension should, in theory, be compatible with this process.

The primary advantage of this technique is that it is a single step process and a complete array of microstructures, either arrays of microcapsules, microchannels or even combinations of both can be fabricated without additional manufacturing steps.

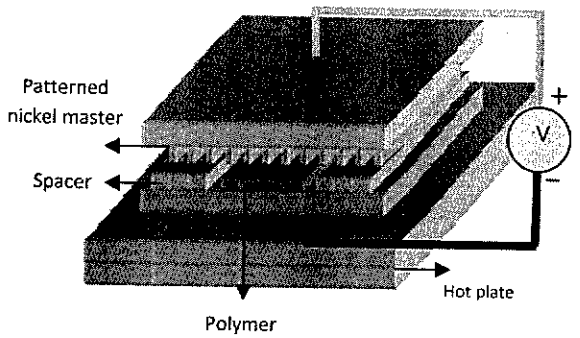

Fig. (3). Schematic of the Experimental Setup.

The size of these arrays is however limited presently by current spin coating technologies as this is used to produce the initial polymer layer, although spray-coating techniques could be implemented. Other limitations include the possible range of sizes of the masks used as electrodes and their costs.

EXPERIMENTAL PROCESS

A schematic of the experimental setup can be seen in Fig. (3). The process starts with a patterned nickel master manufactured using the UV-LIGA process [14]. A glass wafer substrate is then deposited with a multi-layered Ti/Cu/Ti metal thin film. A thin layer of polydimethylsiloxane (PDMS) polymer solution is spin coated onto the substrate. Spacers are used to control the gap between the top electrode and the polymer film.

Alternatively, a high precision placement machine can be employed to control the size of this gap. The manufacturing process is quite simple. Firstly, an AC electric field of 1KV peak-to-peak output voltage is applied to the pre-cured PDMS for an hour to produce the destabilisations in the film and the redistribution of the PDMS monomers. Then a hotplate is used to heat PDMS for 30 minutes at 150°C to cure the polymer and so solidify the microstructure formed in PDMS. After this curing and cooling down to room temperature, the PDMS is separated carefully by hand from the master electrode.

The stages of forming the channels after the experiment has been setup are described in the previous section. It is important to note however that there needs to be sufficient polymer spun coat onto the bottom surface to fully coat the top mask without being depleted.

EXPERIMENTAL RESULTS

Fig. **4** shows scanning electron micrograph images of microcapsules produced using this process. The majority of these capsules can be seen to be hollow. Microstructures of between approximately 50 μm and 350 μm across have been fabricated using this technique however smaller structures should be reproducible with the right sized mask. A thickness of the shell on top of the structure has been observed from a few μm to approximately 30 μm, depending on a number of factors from the amount of polymer at the start and the contact angle of the polymer to the wetted surface.

The technology has also the advantage of producing free-standing structures as the top and bottom electrodes can be detached from the polymer material.

NUMERICAL MODEL

The initial forces on the polymer are the dielectric forces at the interface between the two fluids and gravitational forces. The force at the interface can be calculated from the equation for the force on a dielectric [15]:

$$\mathbf{F} = \rho\,\mathbf{E} - \tfrac{1}{2}\mathbf{E}\cdot\mathbf{E}\nabla\varepsilon + \nabla\left(\tfrac{1}{2}\mathbf{E}\cdot\mathbf{E}\frac{\partial\varepsilon}{\partial_\rho}\rho\right) \qquad \text{Eq. 1}$$

Where **F** is the force density, ρ_f the charge density, **E** the electric field, ε the permittivity and ρ the mass density.

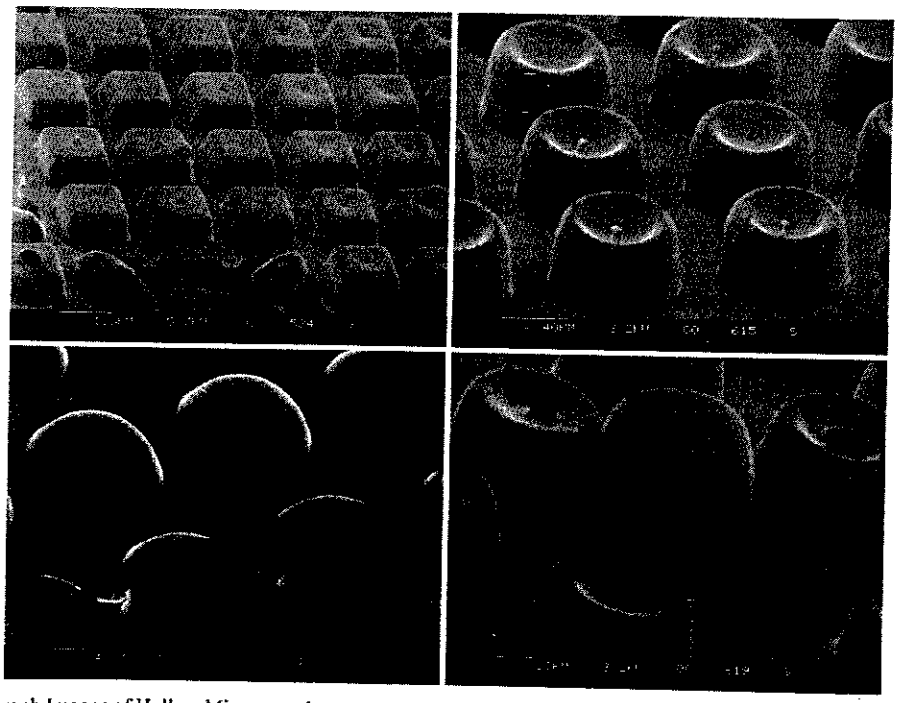

Fig. (4). Electron Micrograph Images of Hollow Microcapsules.

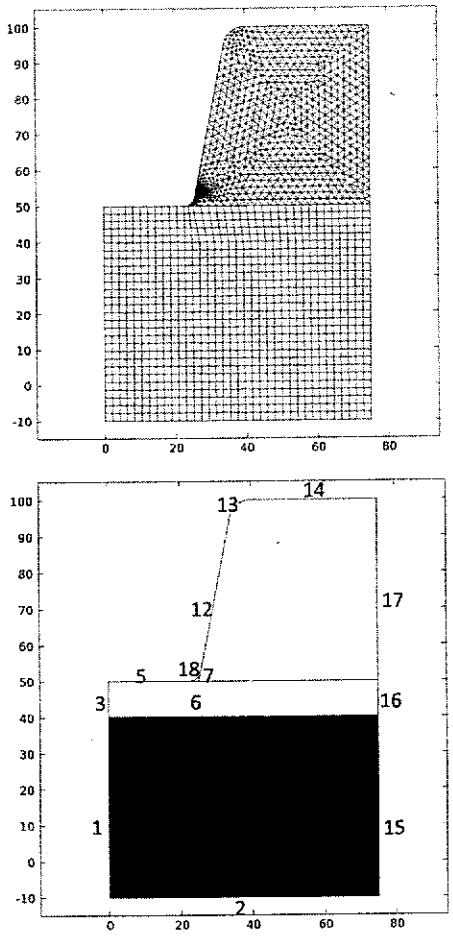

	Flow	Electric Field
1	Slip Wall	Symmetry
2	No-Slip Wall	0V
3	Slip wall	Symmetry
5	Slip wall	300V
6	Wetted Wall	N/A
7	Wetted Wall	N/A
12	Wetted Wall	300V
13	Wetted Wall	300V
15	Symmetry	Symmetry
16	Symmetry	Symmetry
17	Symmetry	Symmetry
18	N/A	300V

Fig. (5). Mesh, Geometry and Boundary Conditions.

The first term in the above equation is simply the electrostatic force in the dielectric. The second term is due to inhomogeneities in the dielectric constant; as both fluids are considered to have a uniform dielectric constant which only has a value at the interface. The final term is the electrostriction force density, which comes from changes in the mass density of the materials, as the fluids are assumed to be incompressible this term only has a value at the interface as the density and permitivity are constant elsewhere.

The polymer is assumed to be a perfect dielectric and has zero free charge in the bulk material. There will however be a charge at the interface due to the change in the dielectric, this can be calculated as [16]:

Table 1. Material Properties of the Polymer

Simulation Dynamic Viscosity (Centipoise)	Specific Gravity (25°C)	Dielectric Constant (100Hz)	Surface Tension (mN/m)
1000	1.03	2.72	20

$$\sigma = (\varepsilon - 1)\varepsilon_0 \mathrm{E} \cdot \hat{} \qquad \text{Eq. 2}$$

Where ε is the relative permittivity of the polymer, ε , the dielectric constant and $\hat{}$ is the unit normal to the interface. As this equation represents the surface charge density it is the charge per unit area. The term ρ_f in equation 1 is however the charge per unit volume and so the normal to the surface is used instead, which is equal to the gradient of the free surface variable. The following equation for the charge density is therefore:

$$\rho = (\varepsilon - 1)\varepsilon_0 \mathrm{E} \cdot \nabla\phi \qquad \text{Eq. 3}$$

where ϕ is the free surface variable substituting equations 2 and 3 into equation 1 gives the overall equation for the force density at the interface as:

$$\mathrm{F} = \varepsilon - 1\ \varepsilon_0 \mathrm{E} \cdot \nabla\phi\ \mathrm{E} \quad \perp \mathrm{E}\nabla\varepsilon + \nabla \perp \mathrm{E} \cdot \mathrm{E}\frac{\partial\varepsilon}{\partial_\rho}\rho \qquad \text{Eq. 4}$$

As there is assumed to be no free charge in the bulk of the material the voltage is solved using the following equation:

$$\nabla\varepsilon\nabla = \rho = 0 \qquad \text{Eq. 5}$$

where V is the voltage.

The interface between the two materials is solved using a phase field free surface technique [17]. A phase field technique was used here as we have found the surface tension calculation is more stable using this technique compared to using a level set technique. The reason for this is that level set techniques use an artificial smoothing function at the interface whereas phase field techniques base the smoothing function on the internal energy of the material. This internal energy at the surface is directly related to the surface tension at the interface between the two fluids and so this can be obtained without the need to calculate the curvature at the surface. The flow is solved using the incompressible form of the Navier Stokes equations in both fluids, this was for numerical stability reasons as we have found the compressible forms would cause the model to become unstable.

The numerical model was implemented in COMSOL Multiphysics 4.2. The Mesh and Boundary Conditions for a typical mask can be seen in Fig. (**5**). At present we are using a two dimensional model which is essentially for an infinite channel, though similar results can be obtained from an axisymmetric model giving a microcapsule. This geometry and mesh is for the results presented in Figs. (**7-9**).

One point to note with this geometry is the curved corner in the top left which was needed in order to achieve a full cap. With an angular corner there would not be enough capillary force to fully coat the mask and the polymer would just get stuck in that corner. The symmetry of the problem has also been exploited with symmetry walls on the left and right hand sides. The problem as described here is essnetially for an infinite plane of microchannels. To decrease the simulation time required an artificially lower viscosity was used. Whilst this was still a high viscosity compared

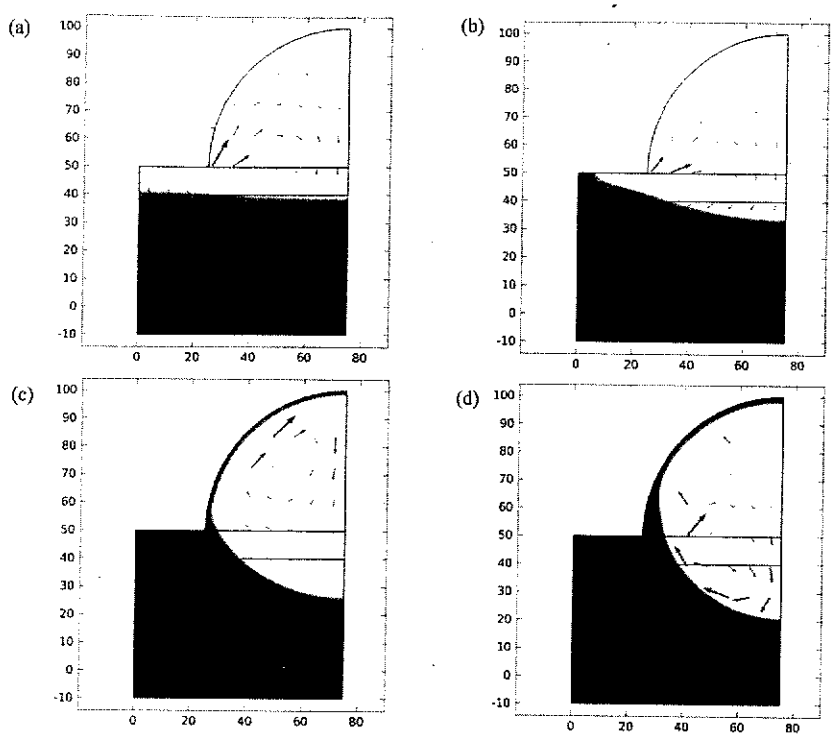

Fig. (6). Evolution of the polymer surface over time for a circular mask, Vectors show the velocities of the fluids.

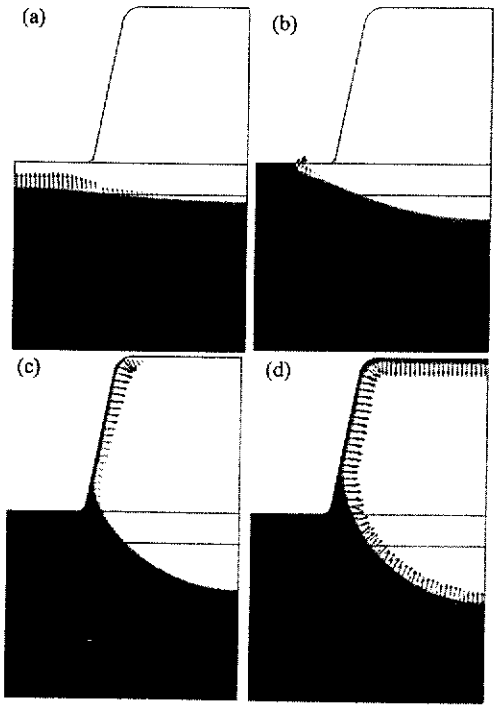

Fig. (7). Evolution of the polymer surface over time for an angular mask, Vectors are the sum of the electrostatic and surface tension forces.

to most materials (for comparison water has a dynamic viscosity of 0.89 cp) it was several times lower than the actual viscosity of the polymer used in the experiments (PDMS) prior to curing. The change of viscosity has the effect of speeding up the simulation speed. However the final results of the cap formed and its thickness have been shown to be the same for different viscosites. The material properties of the polymer can be seen in Table **1**. The properties for air are the default air peroperties within COMSOL.

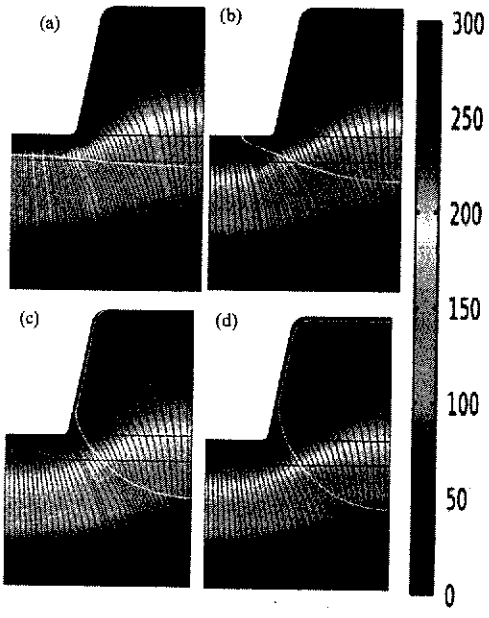

Fig. (8). Evolution of the electric field over time, streamlines show the electric field, The gradient shows voltage and the white contour shows the surface of the polymer.

NUMERICAL RESULTS

Numerical results from the model can be seen in Figs. (**6-9**). The first set of results, shown in Fig. (**6**) produced by Chen *et al.* [3], demonstrate the velocities and also the evolution of the free surface for a curved mask. The surface starts flat (a) and the dielectric force moves the surface upwards until it touches the top mask. At this stage capillary force then causes the polymer film begin to coat the top mask until it eventually reaches the centre (c), and finally the fluid bubble moves due to the electric field almost forming a circle (d). As can be seen from these results the cap thickness is

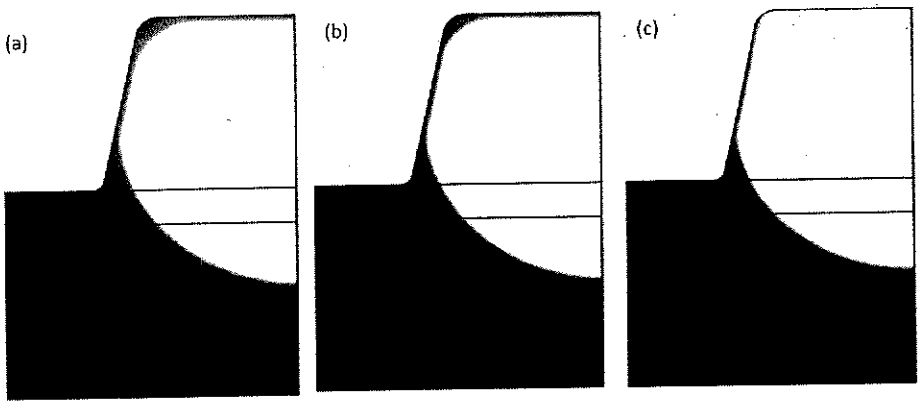

Fig. (9). Comparison of the structures formed by different contact angles for the top mask (**a**) 10 Deg. (**b**) 20 Deg. and (**c**) 25 Deg.

very thin compared to the size of the capsule, which here contains an approximately circular bubble of approximately 150 micron diameter, the shell is approximately 3 microns, this makes it very delicate but it would strengthened by the air pressure due to the bubble trapped inside.

Fig. 7 shows the evolution for an angular mask from results of Tonry *et al.* [16]. The process starts in the same way: as the polymer is pulled up towards the top mask by the dielectric forces (a) once it touches the top mask (b) the capillary force becomes dominant and coats the mask to the corner (c) this then continues round the complete mask (d).

Fig. **8** Shows the evolution of the electric field at the same time points of the surface in Fig. (**6**). Due to the changing dielectric properties caused by the moving surface the electric field changes over time. These diagrams also show the deflection of the electric field at the surface of the polymer.

Fig. **9** shows the effect that the change of wettability of the top mask has on the thickness of the top of the microstructure. A small contact angle creates a thicker microcapsule. The first of these is the thickest and can be seen that the cap here is approximately 5 micron at its thinnest for the 10 degree contact angle, approximately 3 micron for the 20 degree contact angle and a full cap was unable to be formed for the 25 degree case. This is likely due to the reduced capillary force due to the change of wettability of the surface.

Currently the majority of experimental work with EFAC has been performed with air; however as the forces involved are dielectric forces, other dielectric fluids could be substituted and captured within the polymer capsule. As dielectric forces are required for the process to work a conductive fluid cannot be used. The encapsulation of biomolecules should therefore be possible if the molecules are not susceptible to strong electrostatic fields.

PROSPECTS FOR FURTHER STUDY

As the process is currently at a very early stage further work needs to be undertaken in order to fully analyse the methods potential for the fabrication of microstructures.

Firstly the numerical simulations need expanding to take account of some of the physical mechanisms which are currently not considered. The first of these is the fact that the polymer is a non-Newtonian fluid and so its viscoelastic properties may have an effect on the simulation results once implemented. In addition the surface tension properties of a material are modified by being placed in an electric field, this may have an effect on the magnitude of the capillary force and so needs investigating. Also further work is needed to extend the model into three dimensions to provide full results for microcapsules in addition to the work on microchannels.

In addition to this further experiments and simulations need to be undertaken with respect to substituting the air in the capsules for a dielectric fluid.

Another avenue of research is the use of polymers, that are partially permeable to enable the progressive release of material within the capsules.

CONFLICT OF INTEREST

The author(s) confirm that this article content has no conflicts of interest.

ACKNOWLEDGEMENTS

The authors would like to thank the Engineering and Physical Sciences Research Council (EPSRC) for their support for the Modelling work described here which has been funded through a Doctoral Training Award.

REFERENCES

[1] Chang T.M. S.; Prakash S. Procedures for Microencapsulation of Enzymes, Cells and Genetically Engineered Microorganisms, *Molecular Biotechnology*. **2001**, 17, 249-260

[2] Hernández, R. M.; Orive, G.; Murua, A.; Pedraz, J. L. Microcapsules and microcarriers for in situ cell delivery, *Advanced Drug Delivery Reviews*. **2010**, 62, 711-730

[3] Chen, H.; Yu, W.; Cargill, S.; Patel, M. K.; Bailey, C.; Tonry, C.; Desmulliez, M. P. Y. Self-encapsulated hollow microstructures formed by electric field-assisted capillarity, *Microfluidics and Nanofluidics*, **2012**; 13(1), 75-82

[4] Sata, K.; Yoshida, K.; Takahashi, S.; Anzai J. pH- and sugar-sensitive layer-bylayer films and microcapsules for drug delivery, *Advanced Drug Delivery Reviews*, **2011**, 63, 809-821

[5] Whol, B. M.; Engbersen, J. F. J.; Responsive layer-by-layer materials for drug delivery, *Journal of Controlled Release*, **2012**, 158 2-14

[6] Teramura Y.; Iwata H. Bioartifical pancreas Microencapsulation and conformal coating of islet of Langerhans, *Advanced Drug Delivery Reviews*, **2010**, 62, 827-840

[7] Guijt R. M.; Baltussen E.; van der Steen G.; Schasfoort R. B.; Schlautmann, S.; Billiet H. A.; Frank J.; van Dedem G. W.; van den Berg A. New approaches for fabrication of microfluidic capillary electrophoresis devices with on-chip conductivity detection. *Electrophoresis*, **2001**, 22, 235-241

[8] Xia, J.; Qu D.; Yang, H.; Chen, J.; Zhu, W. Self assembly polymer microlens array for integral imaging, *Displays*. **2010**, 31(4-5), 186-190

[9] Barber J. P.; Conkey D. B.; Lee J. R.; Hubbard N. B.; Howell L. L. ; Schmidt, H.; Hawkins A. R. Fabrication of hollow waveguides with sacrificial aluminum cores. *IEEE Photonics Technol Lett*, **2005**, 17, 363-365

[10] Chou S. Y.; Zhuang, L. Lithographically induced self-assembly of periodic polymer micropillar arrays., *Papers from the 43rd international conference on electron, ion, and photon beam technology and nanofabrication*, **1999**. 17(6), 3197-3202

[11] Chou S. Y.; Zhuang, L.; Guo, L. Lithographically induced self-construction of polymer microstructures for resistless patterning. *Applied Physics Letters*. **1999**, 75(7), 1004-1006

[12] Liu, Z.; Kerle, T.; Russel, T. P.; Schäffer E.; Steiner, U. Structure formation at the interface of liquid/liquid bilayer in electric field. *Macromolecules*, **2002**, 35, 6255-6262

[13] Sou, Z.; Liang J. Theory of lithographically induced self-assembly. Applied Physics Leters, **2001**, 78(25), 3971-3973

[14] Qu W.; Wenzel C.; Jahn A.; Zeidler D. UV-LIGA: A Promising and Low-Cost Variant for Microsystem Technology, Precedings of Conference on Optoelectronic and Microelectronic Materials Devices, **1998**, 380-383

[15] Woodson, H. H.; Melcher J. R. *Electromechanical Dynamics, Vol 3: Elastic and Fluid Media;* Wiley & Sons: New York, **1968**

[16] Tonry, C.; Patel, M.; Bailey, C.; Desmuliez, M.P.Y.; Cargill, S.; Yu W. Modelling of the Electric Field Assisted Capillarity Effect used for the Fabrication of Hollow Polymer Microstructures, *Precedings of the 13th Eurosime Conference, Lisbon* 16th-18th April **2012**

[17] Yue, P.; Feng, J. J.; Liu C.; Shen, J. A diffuse-interface method for simulating two-phase flows of complex fluids, *Journal of Fluid Mechanics*, **2004**, 515, 293-317.

Received: August 22, 2012 Revised: September 18, 2012 Accepted: September 19, 2012